

Anomalous Hall effect in $L1_0$ -MnAl films with controllable orbital two-channel Kondo effect

L. J. Zhu*, S. H. Nie and J. H. Zhao†

State Key Laboratory of Superlattices and Microstructures, Institute of Semiconductors, Chinese Academy of Sciences, P. O. Box 912, Beijing 100083, China

Abstract: The anomalous Hall effect (AHE) in strongly disordered magnetic systems has been buried in persistent confusion despite its long history. We report the AHE in perpendicularly magnetized $L1_0$ -MnAl epitaxial films with variable orbital two-channel Kondo (2CK) effect arising from the strong coupling of conduction electrons and the structural disorders of two-level systems. The AHE is observed to excellently scale with $\rho_{AH}/f = a_0\rho_{xx0} + b\rho_{xx}^2$ at high temperatures where phonon scattering prevails. In contrast, significant deviation occurs at low temperatures where the orbital 2CK effect becomes important, suggesting a negative AHE contribution. The deviation of the scaling agrees with the orbital 2CK effect in the breakdown temperatures and deviation magnitudes.

Key words: Anomalous Hall effect, Kondo effect, Strongly correlated electron systems, Magnetic anisotropy

PACS numbers: 75.47.-m, 72.15.Qm, 71.27.+a, 75.30.Gw

* zhulijun0@gmail.com

† jhzhao@red.semi.ac.cn

The anomalous Hall effect (AHE) is the most prominent phenomena existing in magnetic materials. The AHE has received renewed interests in recent years due to its rich phenomenology that defies the standard classification methodology and prompting conflicting reports that claim the dominance of various microscopic processes [1-3]. The scaling between longitudinal resistivity (ρ_{xx}) and anomalous Hall resistivity (ρ_{AH}) can provide access to the detailed mechanisms of the AHE. Present theories predict a scaling of $\rho_{AH} \sim \rho_{xx}^n$, with $n = 2$ for side jump and intrinsic contribution [4,5], and $n = 1$ for skew scattering [6]. The intrinsic contribution is related to the topological Berry curvature of band structure [4], while the extrinsic side jump and skew scattering result from spin-orbit interaction-induced asymmetric impurity scattering of conduction electrons [5,6]. Notably, in contrast to the conventional picture that ρ_{AH} scales with the total resistivity irrespective of its sources [3], recent experimental studies have revealed that both ρ_{AH} and the scaling relation are qualitatively different for various types of electron scattering. Phonon scattering was found to have no distinguishable contribution to extrinsic part of ρ_{AH} in ferromagnetic Fe, Co, Ni, $L1_0$ -Mn_{1.5}Ga films, Co/Pt multilayers, and paramagnetic Ni₃₄Cu₆₆ films [7-12]. When ρ_{xx} is dominated by phonon and static defect scattering, the AHE has a scaling of $\rho_{AH} = a_0\rho_{xx0} + b\rho_{xx}^2$, where ρ_{xx0} is the residual resistivity, $a_0\rho_{xx0}$ is the extrinsic contribution from both side jump and skew scattering, and b is the intrinsic anomalous Hall conductivity (AHC). In magnetic materials with relatively low Curie temperature, the temperature (T) induced variation of the magnetization must be taken into account [13]. For the simplest case that ρ_{AH} scales proportionally with magnetization (M) which is not the fact in some magnetic systems [14,15], the AHE scaling can be modified into a more general expression explicitly as $\rho_{AH}/f = a_0\rho_{xx0} + b\rho_{xx}^2$. Here, $f = M/M_0$, where M_0 is magnetization at 0 K; the T -independence of a_0 and b is not considered. In the presence of strong disorder effects (dirty metal [1]), the AHE scaling is more complex. In the hopping conduction regime, the AHE was reported to scale as $\rho_{AH} \sim \rho_{xx}^{0.4}$ in

Fe_{3-x}Zn_xO₄ and (Ga,Mn)As [16,17], $\rho_{AH} \sim \rho_{xx}^{0.5-0.3}$ in Ti_{1-x}Co_xO_{2- δ} [18], and $\rho_{AH} \sim \rho_{xx}^0$ in polycrystalline FePt [19], respectively. It has remained an open question whether or not weak localization and electron-electron interaction contribute to ρ_{AH} [19-21]. Therefore, further experimental and theoretical attempts are crucial for better understanding of the AHE, especially in disordered magnetic systems.

The Kondo effect is a striking consequence of conduction electrons coupling with localized spin or “pseudospin” impurities. The one-channel Kondo systems are normally found to have an important AHE contribution arising from the coupling of Kondo centers and conduction electrons [22,23]. However, the interplay between the AHE and the two-channel Kondo (2CK) effect displaying exotic non-Fermi-liquid (NFL) physics has remained elusive. Aliev *et al.* predicted an exact cancellation of the AHE contributions from two channels of quadruple 2CK effect when the magnetic field is not so large to eliminate the channel symmetry and presented an experimental evidence in U_{0.9}Th_{0.1}Be₁₃ [24]. In contrast, Sato *et al.* found a negative AHE contribution and a breakdown of the scaling $\rho_{AH} \sim \rho_{xx}^2$ at low T in CeRu₂Si₂ single crystal exhibiting NFL behaviors [25]. To our best knowledge, there have been no reports about the AHE for orbital 2CK effect arising from coherent tunneling scattering of localized “pseudo-spin” 1/2 impurities between two independent quantum wells, i.e. dynamical disorder of structural two-level-systems (TLSs) [26]. The orbital 2CK effect has a magnetic field (H)-independent contribution to ρ_{xx} which scales with $\ln T$ (Kondo scattering), $T^{1/2}$ (NFL regime), and a deviation from $T^{1/2}$ (breakdown of NFL physics) in three characteristic T regimes, respectively.

Most recently, we observed robust and controllable orbital 2CK effect evidenced by the three-regime resistivity increase at low temperatures in $L1_0$ -MnAl ferromagnetic films [27], which may provide an experimental access to the AHE in the presence of the orbital 2CK effect. On the other hand, $L1_0$ -MnAl films are ideal for the AHE studies due to their giant perpendicular

magnetic anisotropy ($\sim 10^6$ erg/cc), well-defined perpendicular hysteresis loops, and large values of ρ_{AH} (e.g. 2~7.5 $\mu\Omega$ cm in $\text{Mn}_{1.5}\text{Al}$ films grown on AlAs-buffered GaAs) [28-32]. However, there has been no report about the temperature dependence of ρ_{AH} or the scaling of the AHE in MnAl to date. In this letter, we present the AHE in $L1_0$ -MnAl epitaxial films with variable orbital 2CK effect. The AHE scaling well agrees with $\rho_{\text{AH}}/f = a_0\rho_{\text{xx}0} + b\rho_{\text{xx}}^2$ in high- T regime where phonon scattering is dominating but seriously breaks down at low temperatures most likely due to a negative AHE contribution of orbital 2CK physics.

A series of 30 nm-thick $L1_0$ -MnAl films with Mn/Al atom ratio of 1.1 were epitaxially grown on semi-insulating GaAs (001) substrates by molecular-beam epitaxy at 200, 250, 300, 350 and 400 °C, respectively, and then capped with a 4 nm-thick Al_2O_3 layer to prevent oxidation [27,30]. The good homogeneity and sharp interface of these films are confirmed by the cross-sectional high-resolution transmission electron microscopy images [29]. More details of structures, magnetic and transport properties could be found elsewhere [27-29]. The values of f of these films were determined by a Quantum Design SQUID-5 system. The films were patterned into 60 μm -wide Hall bars with adjacent electrode distance of 200 μm using photolithography and ion-beam etching for transport measurements (see Fig. 1(a)). Both Hall resistivity ρ_{xy} and ρ_{xx} were measured as a function of T (2-300 K) and perpendicular H by a Quantum Design PPMS-9 system.

Figure 1(b) shows an example of $\rho_{\text{xx}}-H$ curves at different T for $L1_0$ -MnAl films ($T_s = 200$ °C). For all the temperatures concerned in the work, ρ_{xx} varies little with H in comparison to the large value of itself, which is further confirmed by the small magnetoresistance ($< 0.5\%$) [27], suggesting a negligible spin fluctuation and spin waves in this material probably due to their strong anisotropic field [33]. These features hold for all the films with different T_s . Figure 1(c) summarizes ρ_{xx} at $H = 0$ T for all the $L1_0$ -MnAl films as a function of T . Each film shows a resistivity minimum at characteristic temperature (T_m), beyond which ρ_{xx} increases linearly with increasing T due to the dominating phonon scattering. As T decreases from T_m towards 0 K, ρ_{xx} shows an intriguing increase arising from the orbital 2CK effect [27]. More detailed studies show that the values of T_m are about 190, 41, 18, 19, and 24 K for $T_s = 200, 250, 300, 350,$ and 400 °C, respectively [27]. By subtracting the contribution from the orbital 2CK effect, the residual resistivity $\rho_{\text{xx}0}$ (i.e. the offsets $\rho_1 \approx \rho_2$ in ref. 27) was determined to be 218.5, 174.7, 132.2, 135.7, and 141.1 $\mu\Omega\text{cm}$ for the films grown at 200, 250, 300, 350, and 400 °C, respectively.

In order to investigate the AHE and possible interplay with the 2CK effect, we first evaluated ρ_{AH} in $L1_0$ -MnAl films by subtracting the ordinary Hall component R_0H (determined from a linear fit to the high-field regions of the $\rho_{\text{xy}}-H$ curves up to ± 7 T) following the empirical relationship of $\rho_{\text{xy}} = R_0H + R_sM$ with $\rho_{\text{AH}} = R_sM$. Figure 2(a) shows $\rho_{\text{AH}}-H$ curves measured at 300 K for all these films with different T_s . ρ_{AH} and switching field of $\rho_{\text{AH}}-H$ curves show significant variation among these samples, which agrees with the thermally-tuned structural disorders and magnetic

properties [30], Kondo temperature, and the TLS density in these films [27]. The film grown at 200 °C shows the most gradient hysteresis, coinciding with the observation of the strongest orbital Kondo effects among these studied films. Figure 2(b) shows the T profile of ρ_{AH} in these films. ρ_{AH} varies between 1.28 $\mu\Omega$ cm and 1.93 $\mu\Omega$ cm, which is smaller than previously reported 2~7.3 $\mu\Omega$ cm in $\text{Mn}_{1.5}\text{Al}$ films [31,32]. In common magnetic metals, e.g. Fe and $L1_0$ - $\text{Mn}_{1.5}\text{Ga}$ [7,10], ρ_{AH} are always observed to decrease monotonically as T decreases. In striking contrast, ρ_{AH} of our $L1_0$ -MnAl films shows non-monotonic T dependence. For $T_s \geq 300$ °C, as T decreases from 300 K to 2 K, ρ_{AH} first drops monotonically, reaches the minimum around 50 K, and finally climbs up, which is very similar with that in strongly disordered FePt polycrystalline films with hopping conduction [20]. For $T_s = 200$ °C and 250 °C, ρ_{AH} even increases monotonically upon cooling down. So far, there have been few report on similar anomaly in T -dependence of ρ_{AH} [14]. As is shown in Fig. 3(a), with increasing T from 2 K to 300 K, f (here M_0 takes the value at 2 K) changes little for the films grown at beyond 300 °C, whereas reduces by 40% and 50% for the films grown at 250 °C and 200 °C, suggesting a remarkable reduction of Curie temperature. The slightly faster increase in M at lowest temperatures for $L1_0$ -MnAl with $T_s = 200$ °C could be due to possible compensating alignment of Mn atoms at different lattice sites as was widely discussed in chemically disordered MnGa [34,35]. Notably, the corrected anomalous Hall resistivity, ρ_{AH}/f , decreases monotonically with decreasing T (see Fig. 3(b)). However, we infer that the occurrence of orbital 2CK effect at low T could be another reason for such a complex temperature dependence of ρ_{AH} in addition to the T -dependent M , as is further indicated by the scaling behaviors.

To distinguish the different contributions of ρ_{AH} , we checked the scaling behavior of AHE in the $L1_0$ -MnAl in Fig. 3(c). ρ_{AH}/f shows a good linear correlation with ρ_{xx}^2 in the high T regime ($T > T_m$) for all these films with different T_s , consistent with scaling $\rho_{\text{AH}}/f = a_0\rho_{\text{xx}0} + b\rho_{\text{xx}}^2$. The derived values of a_0 and b are summarized in Fig. 4(a) as a function of T_s . a_0 changes from large negative to vanishingly small positive values as T_s increases from 200 °C to 400 °C, which should be due to the reducing extrinsic AHE contribution and static defects, consistent with the observation in $L1_0$ -FePt films [13]. b decreases from $\sim 1.8 \times 10^{-3} \mu\Omega^{-1} \text{cm}^{-1}$ at $T_s = 200$ °C to $6.0 \times 10^{-5} \mu\Omega^{-1} \text{cm}^{-1}$ at high T_s . In the MnAl films with low T_s , the opposite signs of a_0 and b indicate that the extrinsic skew scattering and side-jump contribute to AHC in an opposite way to that of intrinsic contribution as observed in FePt and Fe films [7,13]. The strong T_s dependence of intrinsic AHC b should be attributed partly to the different T dependence of M (see Fig. 3(a)) and partly to the modification of Fermi surface by structural disorders (especially the chemical disorder) [10,13]. As shown in Fig. 4(b), the carrier density p estimated from ordinary Hall coefficient R_0 following the single-band model varies remarkably among the MnAl films with different T_s , confirming the significant variation of the Fermi surface properties with structural disorders. It should be pointed out that the observed variation of b in the samples with the same composition but different degree of structural

disorders reminds us that one should take care when trying to establish the AHE scaling by assuming a constant b or n in a group of samples with different composition.

More intriguingly, the experimental data significantly deviate from the expectation of $\rho_{\text{AH}}/f = a_0\rho_{\text{xx}0} + b\rho_{\text{xx}}^2$ (see Fig. 3(b)) below 150 K and 25 K for $T_s=200$ °C and 250 °C, respectively. For other three samples with $T_m < 25$ K, the breakdown of the scaling law is not evident. The excellent agreement between deviation temperatures of the scaling and T_m below which orbital 2CK effect become important is highly reminiscent of a close relation between this breakdown and the orbital 2CK effect. Importantly, the magnitudes of the deviation at 2 K for different samples are also consistent with their strength (T_K , α , and β in Ref. 27) of the orbital 2CK effect. In fact, such breakdown of the scaling can be readily understood because the 2CK effect gives a positive contribution to ρ_{xx} but a negative or zero contribution to ρ_{AH} [24,25]. Here, there seems a negative contribution to ρ_{AH} of our $L1_0$ -MnAl films below T_m , which is consistent with the observation in quadruple 2CK system of CeRu_2Si_2 single crystal [25]. Unfortunately, the AHE for the 2CK effects is difficult to treat theoretically at present. More theoretical and experimental efforts are needed in the future for better understanding these intriguing AHE scaling behaviors. It should be mentioned that other scaling laws in literature which based on picture that ρ_{AH} scales with the total resistivity irrespective of its sources cannot solve above breakdown problem [36].

In conclusion, we have systematically presented the AHE in ferromagnetic $L1_0$ -MnAl epitaxial films with variable orbital two-channel Kondo effect. The AHE scaling is observed to follow $\rho_{\text{AH}}/f = a_0\rho_{\text{xx}0} + b\rho_{\text{xx}}^2$ at high temperatures where phonon scattering prevails. However, the AHE significantly deviates from it at low temperatures where the orbital 2CK effect becomes important. The breakdown of the scaling seems closely correlated to the orbital 2CK effect which contributes to the longitudinal and anomalous Hall resistivity in different ways. A remarkable tuning of the intrinsic AHC and the carrier density is also observed by varying structural disorders, indicating a significant modification of the Fermi surface properties. These results put forwards new inspiring questions for future theoretical and experimental studies of the AHE.

We acknowledge X. F. Jin for discussions. This work was partly supported by NSFC (Grand No. 61334006) and MOST of China (Grant No. 2015CB921503).

- [1] N. Nagaosa, J. Sinova, S. Onoda, A. H. MacDonald, and N. P. Ong, *Rev. Mod. Phys.* **82**, 1539 (2010).
- [2] D. Xiao, M.C. Chang, and Q. Niu, *Rev. Mod. Phys.* **82**, 1959 (2010).
- [3] P. He, L. Ma, Z. Shi, G. Y. Guo, J. G. Zheng, Y. Xin, and S. M. Zhou, *Phys. Rev. Lett.* **109**, 066402 (2012).
- [4] R. Karplus and J. M. Luttinger, *Phys. Rev.* **95**, 1154 (1954).
- [5] Berger, *Phys. Rev. B* **2**, 4559 (1970).
- [6] J. Smit, *Physica (Amsterdam)* **21**, 877 (1955).
- [7] Y. Tian, L. Ye, and X. F. Jin, *Phys. Rev. Lett.* **103**, 087206 (2010).
- [8] D. Z. Hou, Y. F. Li, D. H. Wei, D. Tian, L. Wu, and X. F. Jin, *J. Phys.: Condens. Matter.* **24**, 482001 (2012).
- [9] L. Ye, Y. Tian, X. Jin, and D. Xiao, *Phys. Rev. B* **85**, 220403 (2012).
- [10] L. J. Zhu, D. Pan, and J. H. Zhao, *Phys. Rev. B* **89**, 220406 (R) (2014).
- [11] F. Zhang, F. S. Wen, Y. F. Lu, W. Li, Y. F. Lu, Z. Y. Liu, B. Xu, D. L. Yu, J. L. He, and Y. J. Tian, *J. Appl. Phys.* **110**, 033921 (2011).
- [12] Y. Li, D. Hou, G. Su, L. Ye, Y. Tian, J. Xu, G. Su, and X. Jin, *Europhys. Lett.* **110**, 27002 (2015).
- [13] M. Chen, Z. Shi, W. J. Xu, X. X. Zhang, J. Du, and S. M. Zhou, *Appl. Phys. Lett.* **98**, 082503 (2011).
- [14] R. Mathieu, A. Asamitsu, H. Yamada, K. S. Takahashi, M. Kawasaki, Z. Fang, N. Nagaosa, and Y. Tokura, *Phys. Rev. Lett.* **93**, 016602 (2004).
- [15] A. Fert, A. Friederich, and A. Hamzic, *J. Magn. Magn. Mater.* **24**, 231 (1981).
- [16] D. Venkateshvaran, W. Kaiser, A. Boger, M. Althammer, M. S. R. Rao, S. T. B. Goennenwein, M. Opel, and R. Gross, *Phys. Rev. B* **78**, 092405 (2008).
- [17] D. Chiba, A. Werpachowska, M. Endo, Y. Nishitani, F. Matsukura, T. Dietl, and H. Ohno, *Phys. Rev. Lett.* **104**, 106601 (2010).
- [18] H. Toyosaki, T. Fukumura, Y. Yamada, K. Nakajima, T. Chikyow, T. Hasegawa, H. Koinuma, and M. Kawasaki, *Nature Mater.*, **3**, 221 (2004).
- [19] Y. M. Xiong, P. W. Adams, and G. Catelani, *Phys. Rev. Lett.* **104**, 076806 (2010).
- [20] A. Langenfeld and P. Wölfle, *Phys. Rev. Lett.* **67**, 739 (1991).
- [21] L. M. Lu, J. W. Cai, Z. Guo, and X. X. Zhang, *Phys. Rev. B* **87**, 094405 (2013).
- [22] G. R. Stewart, Z. Fisk, and J. O. Willis, *Phys. Rev. B* **28**, 171 (1983).
- [23] P. Coleman, P. W. Anderson, and T. V. Ramakrishnan, *Phys. Rev. Lett.* **55**, 414 (1985).
- [24] F. G. Aliev, H. E. Mfarrej, S. Vieira, and R. Villar, *Europhys. Lett.* **34**, 605-610 (1996).
- [25] H. Sato, Y. Aoki, J. Urakawa, H. Sugawara, Y. Onuki, T. Fukuhara, and K. Maezawa, *Phys. Rev. B* **58**, R2933 (R) (1998).
- [26] D. L. Cox and A. Zawadowki, *Adv. Phys.* **47**, 599-942 (1998).
- [27] L. J. Zhu, S. H. Nie, P. Xiong, P. Schlottmann, and J. H. Zhao, *Nat. Commun.* (Accepted); Preprint at arXiv: 1506.04360(2015).
- [28] L. J. Zhu, S. H. Nie, and J. H. Zhao, *Chin. Phys. B* **22**, 118505 (2013).
- [29] S. H. Nie, L. J. Zhu, J. Lu, D. Pan, H. L. Wang, X. Z. Yu, J. X. Xiao and J. H. Zhao, *Appl. Phys. Lett* **102**, 152405 (2013).
- [30] S. H. Nie, L. J. Zhu, D. Pan, J. Lu and J. H. Zhao, *Acta Phys. Sin.* **62**, 178103 (2013).
- [31] J. D. Boeck, T. Sands, J. P. Harbison, A. Scherer, H. Gilchrist, T. L. Cheeks, M. Tanaka and V. G. Keramidias, *Electronics Lett.* **29**, 421 (1993).
- [32] M. L. Leadbeater, S. J. Allen, F. DeRosa, J. P. Harbison, T. Sands, R. Ramesh, L. T. Florez and V. G. Keramidias, *J. Appl. Phys.* **69**, 4689 (1991).
- [33] S. N. Kaul and M. Rosenberg, *Phys. Rev. B* **27**, 5698 (1983).
- [34] L. J. Zhu and J. H. Zhao, *Appl. Phys. A*, **111**, 379-387 (2013).
- [35] L. J. Zhu, S. H. Nie, K. K. Meng, D. Pan, J. H. Zhao, and H. Z. Zheng, *Adv. Mater.* **24**, 4547 (2012).
- [36] See <http://www> for details on the Hall resistivity hysteresis and the fits of the data with conventional scaling laws $\rho_{\text{AH}} \sim \rho_{\text{xx}}^n$ and $\rho_{\text{AH}} = a\rho_{\text{xx}} + b\rho_{\text{xx}}^2$.

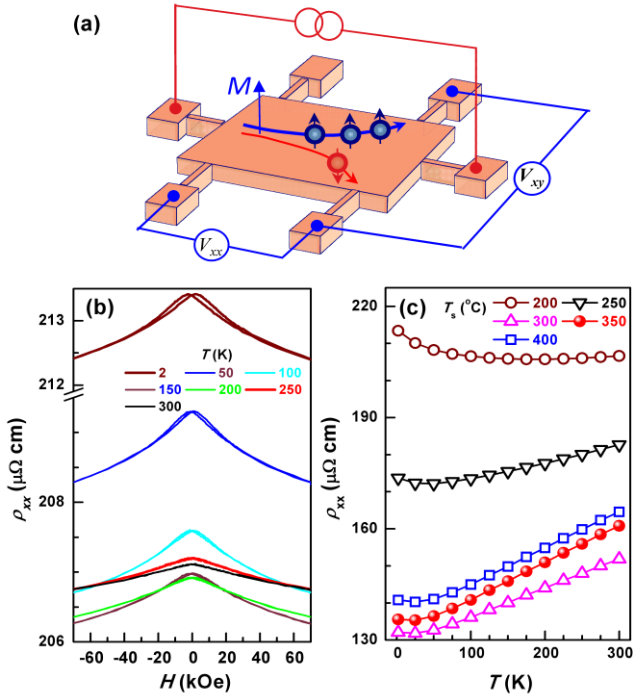


Fig. 1 (a) Schematic of anomalous Hall effect and measurement configuration, (b) ρ_{xx} - H curves ($T_s=200$ °C) and (c) ρ_{xx} - T curves for $L1_0$ -MnAl films with different T_s .

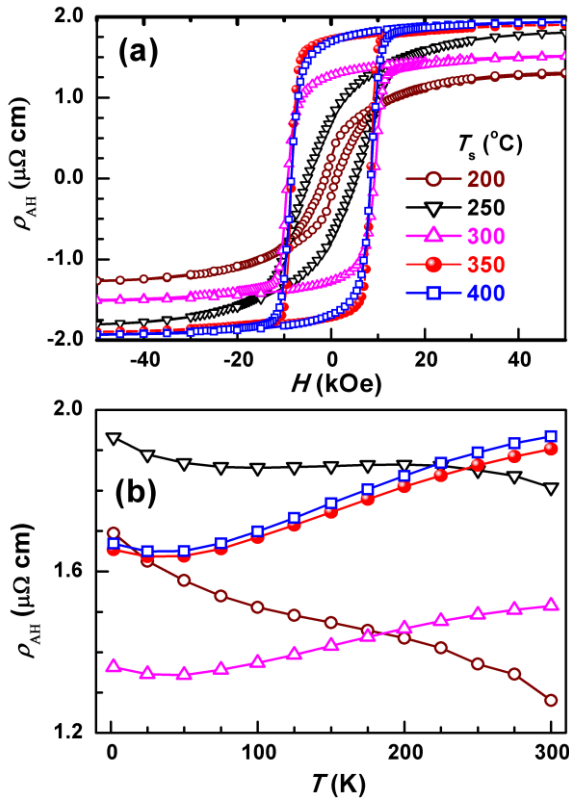


Fig. 2 (a) H (300 K) and (b) T dependence of ρ_{AH} for $L1_0$ -MnAl films grown at 200, 250, 300, 350, and 400 °C.

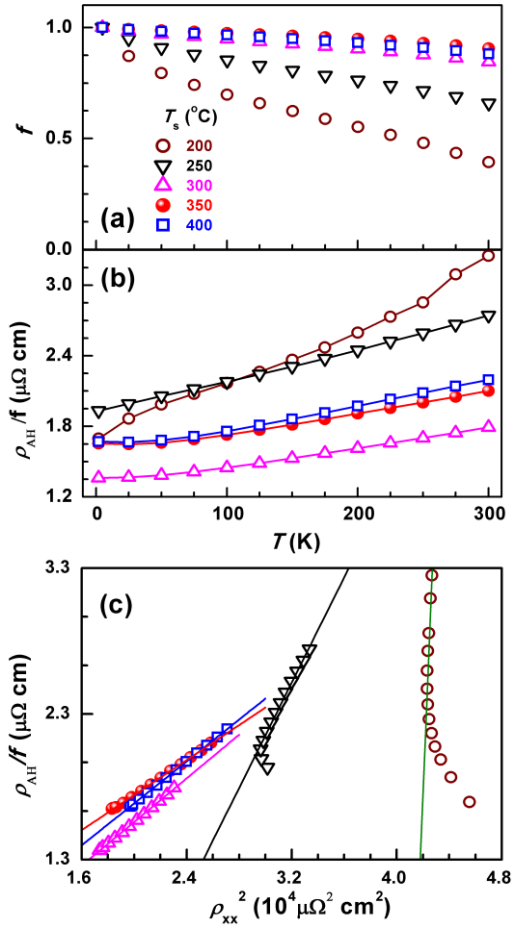


FIG. 3 (a) f versus T , (b) ρ_{AH}/f versus T , and (c) ρ_{AH}/f versus ρ_{xx}^2 for $L1_0$ -MnAl films grown at 200, 250, 300, 350, and 400 °C.

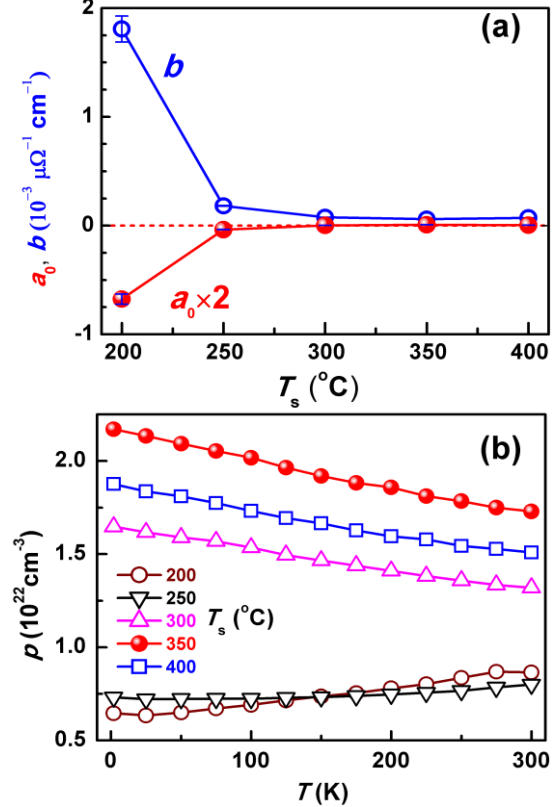


FIG. 4 (a) a_0 , (b) b , and (c) temperature-dependent p for $L1_0$ -MnAl films with different T_s . For clarity, the values of a_0 in (a) is multiplied by a factor of 2.